Magnetic anisotropy of transition-metal dimers: Density functional calculations

Piotr Błoński and Jürgen Hafner*
Fakultät für Physik and Center for Computational Materials Science, Universität Wien, Sensengasse 8/12, A-1090 Wien, Austria
(Received 2 March 2009; revised manuscript received 8 May 2009; published 16 June 2009)

We present *ab initio* density functional calculations of the magnetic anisotropy of dimers of the transition-metal atoms from groups 8 to 10 of the Periodic Table. Our calculations are based on a noncollinear implementation of spin-density functional theory (DFT) where spin-orbit coupling (SOC) is included self-consistently. The physical mechanism determining the sign and magnitude of the magnetic anisotropy energy (MAE) is elucidated via an analysis of the influence of SOC on the spectrum of the Kohn-Sham eigenvalues of the dimers. The possible influence of orbital-dependent electron-electron interactions has been investigated by performing calculation with a hybrid functional (mixing Hartree-Fock and DFT exchanges) and with a DFT+U Hamiltonian introducing an orbital-dependent on-site Coulomb repulsion U. The results demonstrate that the MAE is stable with respect to the addition of such orbital-dependent interactions.

DOI: 10.1103/PhysRevB.79.224418 PACS number(s): 75.30.Gw, 75.75.+a, 36.40.Cg

I. INTRODUCTION

During the 1990s there has been an enormous interest in the magnetic properties of nanostructures, triggered by the rapid development of magnetic and magneto-optic storage technologies.[1] Much of this interest has centered on the question of the minimal size of a bit for classical information storage. The main criterion is that the energy difference between the easy and hard axes of magnetization represents a barrier for spin reorientations exceeding ambient temperatures. An important line of research has centered on molecular magnets[2] but recently there have been suggestions that very small transition-metal clusters might also satisfy this condition.

While the spin-dependent magnetic properties of transition-metal clusters have been widely investigated (see, e.g., Alonso,[3] Baletto and Ferrando,[4] Futschek *et al.*,[5,6] and further references cited therein), only very few *ab initio* investigations have addressed the problem of the magnetic anisotropy of gas-phase[7–9] or supported[10–13] transition-metal clusters. Fernandez-Seivane and Ferrer[8] performed spin-density functional calculations using pseudopotentials and a local basis set [both in the local-density (LDA) and generalized gradient (GGA) approximations] for Pd, Pt, Ir, and Au dimers. For Pd_2 the easy magnetization direction is perpendicular to the dimer axis with a magnetic anisotropy energy (MAE) of 5/2 meV (LDA/GGA) while for Pt_2 and Ir_2 the easy axis coincides with the dimer axis, in which the MAEs are much larger, 220/75 (LDA/GGA) and 100 meV (LDA) per dimer for Pt_2 and Ir_2, respectively. Strandberg *et al.*[7] used a projector-augmented-wave approach in a plane-wave basis and the GGA. They reported perpendicular anisotropy for Pd_2[MAE=2.4 meV(GGA)] and Ni_2(MAE=7 meV), and axial anisotropy for Co_2 and Rh_2 [MAE=30(Co_2) and 45 meV (Rh_2)]. Fritsch *et al.*[9] presented results for a number of 3*d* and 4*d* dimers, calculated using the LDA and a full-potential approach in a basis of numerical localized orbitals. For Pd_2 they agree with the perpendicular anisotropy predicted by the other authors [MAE=5 meV(LDA)]; for Co_2 and Rh_2 their results agree with Strandberg *et al.* on the easy axis but their MAEs are nearly twice as large (50 meV for Co_2 and 104 meV for Rh_2). For Ni_2 axial anisotropy (MAE =11 meV) is predicted in contrast to Strandberg *et al.*[7] In all calculations the MAE is determined as the difference in the total energies of the dimers with different orientations of the magnetic axis. While the calculations of Fernandez-Seivane and Ferrer[8] and of Strandberg *et al.*[7] are based on a scalar-relativistic approach and treat spin-orbit interaction in a self-consistent second-order approximation, the results of Fritsch *et al.*[9] are based on the fully relativistic Dirac equation. Strandberg *et al.* also used the results of the *ab initio* calculations to construct a giant-spin Hamiltonian quantizing the classical anisotropy energy functional. However, it is evident that the available results are too scattered to provide a clear picture of the physical mechanism determining an axial or perpendicular anisotropy or the magnitude of the anisotropy energy.

This is surprising because the calculation of the magnetic anisotropy is a problem of fundamental importance. Magnetic anisotropy, magneto-optical spectra, magnetic dichroism, and other important properties are caused by spin-orbit coupling. Within spin-density-functional theory Bruno[14] and van der Laan[15] have used perturbation theory to derive approximate expressions for the MAE. According to Bruno, for a system where the majority-spin band is completely filled, the MAE is proportional to the spin-orbit coupling (SOC) parameter ξ and to the difference in the expectation values of the orbital moment calculated for the easy and hard axes of magnetization (i.e., to the anisotropy of the orbital moment). van der Laan derived in addition a correction term which is second order in ξ and which accounts in addition for a possible anisotropy of the spin moment.

Whereas the spin magnetic moments are described quite accurately by density functional theory, the orbital moments are generally underestimated. The reason is that the variables determining the effective one-electron potential within density functional theory (the charge and spin densities) are determined as averages over occupied orbitals. For small transition-metal clusters supported on nonmagnetic substrates where the small MAE has been calculated using the force theorem or the torque force approach,[10–13] the results are generally in good qualitative and semiquantitative agreement with Bruno's and van der Laan's models. An exception

are, as recently pointed out by Andersson *et al.*,[16] magnetic nanostructures supported on or sandwiched by late 4*d* or 5*d* transition metals with a strong spin-orbit coupling. In these cases off-site spin-orbit coupling between the *d* states across the interface makes a dominant contribution to the MAE. The situation remains unclear for gas-phase clusters. In the studies published so far, the MAE has been calculated in terms of the difference in the total energies of two independent self-consistent calculations—the results should hence be more reliable than those based on the use of the force theorem. However, since only Fritsch *et al.*[9] report detailed results on the spin and orbital moments (but no spin-orbit coupling parameters), the validity of the perturbation formulas for the transition-metal dimers is difficult to asses—but at least for Pd_2 a larger orbital moment for parallel magnetization and an easy axis perpendicular axis are in contradiction to the perturbation treatment.

For the magnetic anisotropy of small clusters the size of the orbital moment becomes of decisive importance. Solovjev[17] has pointed out that orbital magnetism is essentially an atomic phenomenon, as it is proportional to the gradient of the effective one-electron potential which is large only in a small region around the nucleus. Many attempts have been made to devise orbital polarization corrections to the density functional Hamiltonian—an exchange-correlation field which couples to the orbital magnetic moment. The empirical orbital polarization term proposed by Brooks *et al.*[18,19] has recently been discussed by Eschrig *et al.*[20] within fully relativistic current-density functional theory, and by Solovjev[17] and Chadov *et al.*[21] in connection with the more general LDA+U (Ref. 22) and dynamical mean-field theory.[23] While the orbital polarization corrections give a fairly accurate description of orbital moment in bulk 3*d* magnets,[24] they tend to overestimate the orbital moments of dilute 3*d* impurities in noble-metal matrices[22,25] or of 3*d* adatoms on noble-metal substrates.[11,12] For the impurity cases Chadov *et al.*[21] demonstrated that an LDA+dynamic mean field theory (DMFT) approach with a modest on-site Coulomb repulsion of $U=3$ eV leads to values of the orbital moment intermediate between the LDA and orbital polarization approaches, and in better agreement with experiment. Fritsch *et al.*[9] investigated the influence of an orbital polarization contribution to the Hamiltonian on the orbital moments, and on the MAE of 3*d* and 4*d* dimers. For most of the late transition metals the orbital polarization corrections lead to a significant enhancement of the orbital magnetic moments and to a dramatic increase in the MAE. However in some cases (as for the Fe dimer) even if the anisotropy of the orbital moments is decreased, a pronounced increase in the MAE by a factor of 5 is reported. For Pd_2, orbital polarization changes the sign of the MAE which remains, however, an order of magnitude smaller than for Fe, Co, Ni, and Rh dimers where the inclusion of orbital polarization terms leads to MAEs varying between 150 and 200 meV. In contrast for dimers of the early transition metals, the correction terms have only a very modest influence on the orbital moments and leave the MAEs almost unchanged. This is surprising because the earlier work of the same group[20] had reported similar orbital polarization corrections to the total energies of the divalent cations of early and late 3*d* transition elements.

The magnetic properties of transition-metal dimers are of course closely related to those of infinite metallic chains—after all, dimers can be considered as short pieces of such chains. Although many investigations have been devoted to the magnetic order of such chains (see, e.g., Spišák and Hafner[26] and Mokrousov *et al.*,[27] and further references cited therein), only fewer studies have addressed the problem of their magnetic anisotropy.[28–33] For free-standing wires formed by the magnetic 3*d* transition metals, it has been shown[28,29,31] that the size of the orbital moment and the magnetic anisotropy energy depend very sensitively on the exact geometry of the wire (interatomic distances, straight or zigzag wire). Although the orbital moment increases with a decreasing dimensionality (from bulk to monolayer and to monowires), at equilibrium the values remain smaller than expected on the basis of x-ray circular dichroism experiments on supported monowires. Adding an orbital polarization term to the DFT Hamiltonian leads to a huge increase in the orbital moment (by a factor of 5 for Co wires) to values that are evidently too large.[28,29] Desjonquères *et al.*[33] studied the formation of orbital moments within a Hartree-Fock decoupling scheme and simpler Hamiltonians with and without orbital polarization corrections. It was concluded that the orbital polarization corrections are convenient and reliable for systems with saturated magnetic moments only. Intriguing results have been reported for the orbital moments and magnetic anisotropy energies of wires formed by 4*d* or 5*d* transition metals.[30,32] It was shown that the equilibrium interatomic distances are very close to the onset of magnetism in these wires; at equilibrium the spin moments are about μ_B, $0.2\mu_B$, and $0.5\mu_B$ in Ru, Rh, and Pd, the orbital moments are about $0.17\mu_B$, $0.37\mu_B$, and 0 for axial, and $0.05\mu_B$, 0, and $0.12\mu_B$ for perpendicular magnetization for the same series of metals. The large orbital anisotropies are reflected in large MAEs although with no proportionality between orbital anisotropy as expected from perturbation theory. Stretched nanowires display a dramatic increase in both spin and orbital moments, and reversal in the sign of the MAE without a change in the sign of the orbital anisotropy.[30] For Pt monowires is has been reported[32] that at equilibrium both spin and orbital magnetic moments exist only for parallel, but not for perpendicular, orientation of the magnetization—in such a case the MAE is determined by the energy difference between a magnetic and a nonmagnetic wire, and consequently is very large. However, at these distances the magnetic moments are still very small ($\mu_S \sim \mu_L \sim 0.2\mu_B$).

Here we present density functional calculations of the magnetic anisotropy energies for dimers of the Fe, Co, and Ni groups. Our aim is to study systematic trends in the MAE as a function of the filling of the *d* band and through a series of homologous elements from the 3*d* to the 5*d* series and to elucidate the mechanisms determining the sign and the magnitude of the MAE. In addition we briefly investigate the influence of postdensity-functional approximations (LDA+U, hybrid functionals) on orbital moments and magnetic anisotropy.

II. COMPUTATIONAL DETAILS

We have used the Vienna *ab initio* simulation package (VASP) (Refs. 34 and 35) to perform *ab initio* electronic struc-

ture calculations and structural optimizations. VASP performs an iterative solution of the Kohn-Sham equations of density functional theory within a plane-wave basis and using periodic boundary conditions. A semilocal functional in the GGA (Ref. 36) (PW91) and the spin interpolation proposed by Vosko *et al.*[37] is used to describe electronic exchange and correlation and spin polarization. The use of a semilocal functional is known to be essential for the correct prediction of the ground state of the ferromagnetic $3d$ elements in the bulk.[38] The projector-augmented wave (PAW) method[35,39] is used to describe the electron-ion interactions. The PAW approach produces the exact all-electron potentials and charge densities without elaborate nonlinear core corrections—this is particularly important for magnetic elements.

The PAW potentials have been derived from fully relativistic calculations of the atomic or ionic reference calculations. Spin-orbit coupling has been implemented in VASP by Kresse and Lebacq.[40] Following Kleinman and Bylander[41] and MacDonald *et al.*[42] the relativistic Hamiltonian given in a basis of total angular-momentum eigenstates $|j,m_j\rangle$ with $j=l\pm\frac{1}{2}$ (containing all relativistic corrections up to order α^2, where α is the fine-structure constant) is recast in the form of 2×2 matrices in spin space by reexpressing the eigenstates of the total angular momentum in terms of a tensor product of regular angular-momentum eigenstates $|l,m\rangle$ and the eigenstates of the z component of the Pauli-spin matrices. The relativistic effective potential consists of a term diagonal in spin space which contains the mass velocity and Darwin corrections, and the spin-orbit operator,

$$\mathbf{V}=\mathbf{V}^{\mathrm{sc}}+\mathbf{V}^{\mathrm{SO}}=\sum_{l,m}[V_l\cdot 1_\sigma+V_l^{\mathrm{SO}}\vec{L}\cdot\vec{\mathbf{S}}]|l,m\rangle\langle l,m|.$$

where 1_σ is the unit operator in spin space and

$$\vec{L}\cdot\vec{\mathbf{S}}=\frac{1}{2}\begin{pmatrix}L_z & L_-\\ L_+ & -L_z\end{pmatrix}.$$

The l components of the scalar V_l and spin-orbit V_l^{SO} potentials are weighted averages over the $l\pm\frac{1}{2}$ components. The Hamiltonian is therefore a 2×2 matrix in spin space. The nondiagonal elements arise from the spin-orbit coupling but also from the exchange-correlation potential when the system under consideration displays a noncollinear magnetization density. Calculations including spin-orbit coupling have, therefore, to be performed in the noncollinear mode implemented in VASP by Hobbs *et al.*[43] and Marsman and Hafner.[44]

In our calculations, the dimers have been placed into a large cubic box with an edge of 10 Å—this ensures that the separation between the periodically repeated images of the dimer is large enough to suppress any interactions. The basis set contained plane waves with a maximum kinetic energy of 500 eV. For a Co dimer test calculations have been performed with cutoff energies varying between 250 and 700 eV, leading to magnetic anisotropy energies of 7.49/7.09/7.20 meV for cutoff energies of 250/500/700 eV, indicating that a cutoff of 500 eV is a reasonable compromise between accuracy and computational effort. The calculations have been performed in two steps. First a collinear scalar-relativistic calculation has been performed, producing the correct geometry for a spin eigenstate. In those cases where there are reasons to suspect the coexistence of different spin isomers with only small differences in the total energy, fixed-moment calculations were performed for the competing spin isomers to uniquely determine the ground state. The ground state resulting from the scalar-relativistic calculations was used to initialize the noncollinear calculations including spin-orbit coupling. For each dimer at least three calculations have been performed to find the easy and hard magnetic axes and to determine the MAE. In the first two calculations, the direction of the magnetic axis was initialized along the dimer axis (chosen along [001]) or parallel to the equatorial plane of the dimer, i.e., along [100]. By symmetry, the total energy is stationary for magnetic moments in these two orientations. To cross-check the results, a third calculation was initialized with an oblique angle between the magnetic moment and the axis, and the equatorial plane of the dimer (usually the initialization was along the [111] direction). In these calculations the direction of the magnetic moment relaxed into the easy axis, and usually the difference in the total energy for easy-axis orientation was smaller than 0.01 meV. Spin-orbit coupling mixes different spin eigenstates. To control the importance of the initial value of the magnetic moment, parallel calculations have been performed. In a few cases different initializations led to different relativistic ground states—details will be discussed below. Geometric, electronic, and magnetic degrees of freedom are relaxed simultaneously until the change in total energy between successive iteration steps are smaller than 10^{-7} eV—such a stringent relaxation criterion was found to be absolutely essential.

Orbital magnetic moments are calculated directly from the wave functions as the expectation value of the components of the angular-momentum operator along the direction of magnetization. Within the group of $3d$ and $4d$ metals we observe the same trend: the orbital moment increases from Fe_2 to Co_2 and from Ru_2 to Rh_2, to decrease again in Ni and Pd dimers. This variation follows roughly the trend in the orbital moments of the isolated atoms as given by Hund's rule.

The MAE consists of two contributions: the difference in the total electronic energies for easy and hard magnetization directions induced by the spin-orbit coupling, and the magnetostatic (or shape) anisotropy to the magnetic dipolar interactions. The shape anisotropy is zero in cubic solids, usually negligible even in anisotropic solids but often relevant in ultrathin magnetic films[45] where it can trigger a magnetic reorientation transition. For monowires Tung and Guo[31] have reported a shape anisotropy which is considerably smaller than the electronic contribution. We have calculated the dipolar interaction energy for all dimers—the contributions are of the order of 0.1 meV and hence again negligible compared to the electronic term.

In addition to the DFT calculations at the GGA level, we also performed a few test calculations with hybrid functionals mixing density functional and exact (Hartree-Fock) exchange, and using the DFT+U method. The PBE0 (Ref. 46) and HSE03 (Ref. 47) functionals have been implemented in VASP by Paier *et al.*,[48] and we refer to their paper for all further details. The LDA+U approach[22] has been implemented in VASP by Rohrbach *et al.*[49] Both in the DFT+U and

TABLE I. Interatomic distance d (in Å), spin multiplicity $2S+1$ from scalar-relativistic calculations, spin μ_S and orbital μ_L moments from calculations including spin-orbit coupling (in μ_B) of transition-metal dimers for axial and perpendicular orientations of the magnetization, magnetic anisotropy energy (MAE), and spin-orbit coupling constant ξ (both in meV). The MAE is positive for any easy axis parallel to the dimer axis.

				Axial		Perp.			
Dimer		d	$2S+1$	μ_S	μ_L	μ_S	μ_L	MAE	ξ
Fe_2	PW[a]	1.98	7	5.84	0.32	5.84	0.16	0.3	24
	FKRE[b]	1.96	7	6.00	1.89	6.00	0.19	32.0	
Ru_2	PW	2.07	5	3.98	0.00	3.94	0.24	−36.5	334
Os_2	PW	2.10	5	3.75	−0.80	3.48	0.62	28.8	885
Co_2	PW	1.96	5	3.90	0.78	3.90	0.32	7.1	32
	FKRE	1.94	5	4.09	2.00	4.14	0.33	50.0	
	SCM[c]	1.98						28.0	85
Rh_2	PW	2.21	5	3.86	1.82	3.80	0.50	47.3	136
	FKRE	2.21	5	3.98	2.12	3.93	0.63	104.0	
	SCM	2.22	5					52.0	140
Ir_2	PW	2.22	5	3.88	1.96	3.42	0.94	69.8	413
	FSF[d]	2.22		4.00	1.34	4.10	1.24	100.0	
Ni_2	PW (A)	2.09	3	1.98	0.58	1.96	0.38	6.5	101
	PW (B)	2.09	3	1.98	0.12	1.98	0.38	−5.9	
	FKRE	2.05	3	1.99	0.88	1.99	0.45	11.0	
	SCM	2.10	3					−7.6	
Pd_2	PW	2.49	3	1.96	0.02	1.98	0.36	−2.3	404
	FKRE	2.93	3	1.94	0.86	1.98	0.53	−5.0	
	FSF	2.45		2.00	0.02	1.96	0.56	−2.0	
		(2.53)		(2.00)	(0.02)	(2.00)	(0.44)	(−5.0)	
	SCM	2.50	3					−1.2	
Pt_2	PW	2.38/2.35[e]	3	1.88	2.74	1.34	0.80	46.3	742
	FSF	2.38		1.90	2.40	1.65	1.20	220.0	
		(2.45)		(1.95)	(2.40)	(1.75)	(1.10)	(75.0)	

[a]Present work (GGA).
[b]Fritsch *et al.*, Ref. 9 (LDA).
[c]Strandberg *et al.*, Ref. 7 (GGA).
[d]Fernandez-Seivane and Ferrer, Ref. 8 (LDA, GGA in parentheses).
[e]Different dimer lengths for axial and perpendicular magnetizations, cf. text.

the hybrid functional approaches the exchange-correlation potential is orbital dependent and it is interesting to explore whether this changes the results derived from conventional DFT calculations.

III. RESULTS

Our results for the bond length, spin and orbital moments in axial and perpendicular orientations, magnetic anisotropy energy, and spin-orbit coupling strength are compiled in Table I. As far as available, results from the earlier studies of Fritsch *et al.* (FKRE in the following),[9] Strandberg *et al.* (SCM in the following),[7] and Fernandez-Seivane and Ferrer (FSF in the following) (Ref. 8) are also listed for comparison. But it has to be emphasized that in the paper by FSF, the values of the magnetic moments and of the bond length can be read only from small graphs, and that SCM (Ref. 7) have reported slightly different values for the MAE in their two publications. For the metals of the Co group the easy magnetic axis is always parallel to the dimer axis; the MAE increases strongly from Co_2 to Ir_2 with increasing strength of the spin-orbit coupling. In the Fe group we find a very small axial anisotropy for Fe_2, a strong perpendicular anisotropy for Ru_2, and a modest axial anisotropy for Os_2. In the Ni group the trend is also quite complex: we calculate an axial anisotropy for Ni_2 and Pt_2 (much stronger for the Pt dimer as expected from the strength of the spin-orbit coupling), but a weak perpendicular anisotropy for Pd_2. In the following sections we shall attempt to explain the variation in the MAE with band filling and increasing strength of relativistic effects in terms of a detailed analysis of their eigenvalue spectra. We begin with the Co group where the situation is relatively simple. The contributions of the magnetostatic dipolar interactions to the MAE have been calculated for all dimers. For the dimers of the 3*d* metals where the magnetic moments are

largest, the dipolar contributions to the MAE are −0.26, −0.16, and −0.04 meV/dimer for Fe_2, Co_2, and Ni_2. Except for the Fe dimer where the dipolar contribution leads to a further reduction in an already exceptionally very weak MAE, these values are entirely negligible compared to the electronic terms to which our attention is therefore restricted in the following.

A. Co group

All dimers of the metals of the Co group have the easy magnetic axis oriented along the dimer axis. The scalar-relativistic calculations lead to a ground state with $S=2$ for all three dimers. Adding SOC leaves the interatomic distance unchanged for Co_2 and Rh_2; only for the Ir dimer does the bond length increase by 0.01 Å. SOC mixes different spin eigenstates; this leads to a slight reduction in the magnetic spin moment which becomes more pronounced with increasing strength of the SOC. For Rh_2 this agrees with the results of FKRE (Ref. 9) but for Co_2 they predict an even slightly increased magnetic spin moment. A strong SOC also induces an anisotropy of the spin moment, $\Delta\mu_S=(0.0/0.06/0.46)\mu_B$ for Co/Rh/Ir, with a larger spin moment for easy-axis orientation. A much stronger anisotropy is calculated for the orbital magnetic moment, $\Delta\mu_L=(0.46/1.32/1.02)\mu_B$. For perpendicular magnetization our calculated orbital moments are in reasonable agreement with FKRE (Ref. 9) but they report larger orbital moments for parallel magnetization (in particular for Co_2). FSF (Ref. 8) report essentially a very small anisotropy of both spin and orbital magnetic moments for Ir_2—which is surprising since they also report a large MAE of 100 meV. Our calculations permit in principle a noncollinear orientation of spin and orbital moments but we always find a strictly collinear orientation.

For the Co_2 dimer our calculated MAE of 7.1 meV is substantially lower than the results reported by SCM (Ref. 7) and by FKRE.[9] The disagreement with SCM (who also reported a much stronger SOC of 85 meV) is particularly intriguing because their calculations have also been performed using the VASP code. For this reason we have checked very carefully all computational parameters. Varying the plane-wave cutoff between 250 and 700 eV left both spin and orbital moments unchanged; the calculated MAE varied only by ±0.2 meV. A different initialization of the magnetic moment also leads to the same results. Initializing the direction of the magnetic moment in an oblique direction led to convergence to the easy axis, with a difference in the total energies smaller than 0.01 meV for all values of the cutoff energy. It is difficult to asses the reasons for the discrepancy with SCM because no results for the magnetic moments and only selected details of the computational setup have been reported. Their cutoff energy was 348 eV but the decisive difference could be the criterion for terminating the self-consistent iterations. We have found that relaxing the criterion for total-energy convergence from 10^{-7} eV can lead to substantial changes in the MAE.

For a Rh_2 dimer on the other hand we note very good agreement with SCM.[7] FKRE (Ref. 9) report slightly larger spin and orbital magnetic moments and orbital anisotropy

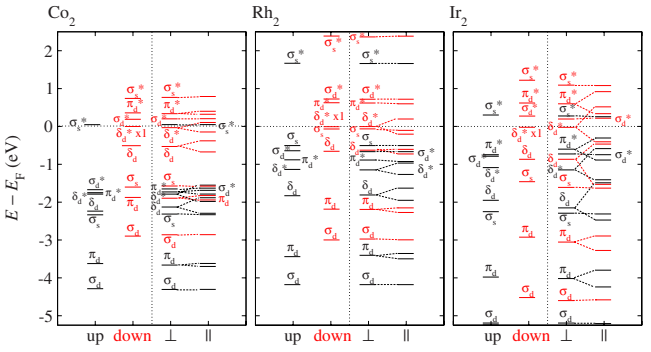

FIG. 1. (Color online) Kohn-Sham eigenvalue spectra for Co_2 (left), Rh_2 (center), and Ir_2 (right) dimers. The left-hand part of each graph shows the spin-up (black) and spin-down (red/gray) eigenvalues from the scalar-relativistic calculations while the right-hand part shows the eigenvalues for parallel and perpendicular orientations of the magnetic moment after adding spin-orbit coupling. The coloring is the same as for the scalar-relativistic eigenstates from which the fully relativistic states are derived (although they are of course not spin eigenstates). The eigenvalues refer to states with quantum numbers $m_J=m_L\pm\frac{1}{2}$.

but these differences are hardly sufficient to explain an MAE which is larger by a factor of 2. For Ir_2 the orbital anisotropy is reduced compared to Rh_2 but here we note also a rather pronounced anisotropy of the spin moment. The reduced orbital anisotropy could explain that the MAE does not increase as strongly compared to the lighter homologs as the strength of the SOC would suggest. For Ir_2 FSF (Ref. 8) report an even larger MAE but with nearly isotropic-spin and orbital magnetic moments.

It is also interesting to correlate the calculated MAEs with the perturbation theories proposed by Bruno[14] and van der Laan.[15] For Co_2 and Rh_2, where the spin anisotropy vanishes or is very small, Bruno's expression ($\mathrm{MAE}\propto\xi\mu_S\Delta\mu_L$) predicts an MAE which should be about 12 times larger for Rh_2 than for Co_2 whereas we find only an increase by a factor of 7. For Ir_2 we note a substantial anisotropy of the spin moment so that Bruno's formula cannot be expected to be valid. van der Laan's approximate expression for the MAE accounts for the spin anisotropy but only in the limit of a weak SOC—which is evidently not the case for Ir_2.

To analyze the reason for the strong axial MAE in the dimers of the Co-group metals, we follow SCM (Ref. 7) in analyzing the Kohn-Sham eigenvalue spectra of the dimers in the scalar-relativistic mode, and after adding SOC for parallel and perpendicular orientations (see Fig. 1). In the scalar-relativistic approximation, the eigenvalue spectrum of the dimer is determined by the electronic ground state of the isolated atom (s^2d^7 for Co and Ir, sd^8 for Rh), and the bonding-antibonding and exchange splittings. In all three dimers the highest occupied molecular orbital (HOMO) is a doubly-degenerate antibonding $\delta_d^\star$ minority (spin-down) state occupied by one electron only. For the Co_2 dimer where the exchange splitting is largest, the highest occupied majority state is the antibonding $\sigma_d^\star$ state but the antibonding $\delta_s^\star$ and $\pi_d^\star$ states lies just below the majority HOMO. For Rh_2 the different atomic ground state leads to an up shift of the s states relative to the d states; the highest occupied majority

state is now the bonding σ_s state. For the Ir_2 dimer the ordering of the minority levels is the same as for Co_2 but with an increased bonding-antibonding splitting and a decreased exchange splitting. For the majority states the highest occupied level is now the $\pi_d^\star$ state. SOC leads to a lifting of the twofold degeneracy of the δ_d and π_d states if the magnetization is parallel to the dimer axis. For the HOMO $\delta_d^\star$ the SOC splitting is 0.94 eV in Ir_2, 0.41 eV for Rh_2, and 0.26 eV for Co_2. The lowering of the occupied $\delta_d^\star$ states (by −0.39 eV for Ir_2) is the dominant effect determining the MAE. A similar splitting is observed also for all other doubly-degenerate eigenstates but in most cases the SOC splitting does not change the average energy—an exception are again the fully occupied $\delta_d^\star$ and δ_d states whose center of gravity is up shifted for Ir_2 by 0.13 and 0.20 eV, respectively. Taking the sum over the change in the eigenvalues yields an energy difference of 0.06 eV—in almost perfect agreement with the calculated MAE. However, this degree of agreement is a bit accidental; for Rh_2 the difference in the sum over the eigenvalues is 0.1 eV, somewhat larger than the calculated MAE. For Co_2 the eigenvalue analysis gives only a qualitative indication of the sign of the MAE; the small value requires an accurate calculation of the total-energy difference.

B. Ni group

For Ni_2 our calculations lead to two locally stable solutions with equal bond length and almost equal spin moments but widely different orbital moments for an axial orientation of the magnetization. For solution A, the orbital moment is $\mu_L=0.58\mu_B$ for axial, and $\mu_L=0.38\mu_B$ for perpendicular orientation. In this case we predict an easy axis parallel to the dimer axis and a modest MAE of 6.5 meV, in reasonable agreement with FKRE.[9] For solution B, the orbital moment is $\mu_L=0.12\mu_B$ for axial, and $\mu_L=0.38\mu_B$ for perpendicular orientation. This is also the easy axis, with an MAE of −5.9 meV, in agreement with SCM (Ref. 7) who also found a perpendicular anisotropy. The total energy for easy-axis orientation is lower by 27 meV for solution A which represents the ground state.

For Pd_2 all calculations are in agreement on a perpendicular easy axis, a weak orbital anisotropy, and a modest negative MAE of a few meV although FKRE predict a much larger orbital moment for the hard magnetic axis. For Pt_2 we predict a parallel easy axis, in good agreement with the GGA result of FSF (Ref. 8) whose LDA calculations yield, however, a much higher MAE. Both calculations also agree on a substantial spin anisotropy. We shall again attempt to analyze the origin and magnitude of the magnetic anisotropy in terms of an analysis of the eigenvalue spectra (see Fig. 2).

For the dimers of the Ni-group metals the ground state is a triplet ($S=1$) state but the Kohn-Sham eigenvalue spectra differ already at the scalar-relativistic level due to the different electronic configurations of the free atoms in their ground state. Ni has a s^2d^8 ground state. The doubly-degenerate minority $\delta_d^\star$ state occupied by two electrons is the HOMO; the highest occupied majority state has the same symmetry. The occupied bonding σ_s state lies almost in the center of the d states. Pd has a closed-shell d^{10} ground state, i.e., formation

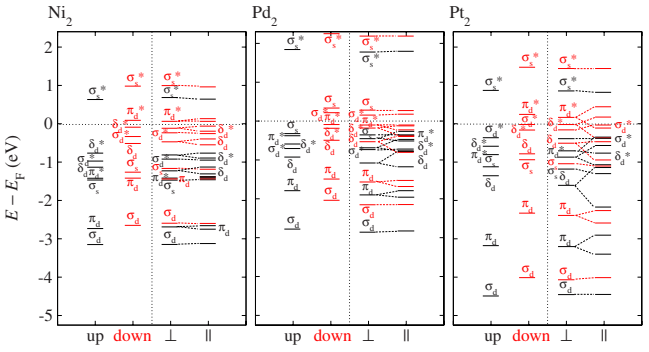

FIG. 2. (Color online) Kohn-Sham eigenvalue spectra for Ni_2 (left), Pd_2 (center), and Pt_2 (right) dimers, cf. Fig. 1.

of a stable dimer requires a promotion of at least one d electron to an s state—this is also reflected in a low binding energy of the dimer. The HOMO is the fully occupied doubly-degenerate $\pi_d^\star$ minority state while the lowest unoccupied molecular orbital is the minority $\sigma_d^\star$ state. The highest occupied majority state is σ_s. This means that the excess spin density arises from the bonding σ_s state and a hole in the d state of $\sigma_d^\star$ character. A Pt atom has a sd^9 ground state. For the dimer the HOMO is the minority $\sigma_d^\star$ state; the highest majority state has the same symmetry. For the minority electrons, an antibonding $\delta_d^\star$ lies only slightly below and an empty $\pi_d^\star$ state only slightly above the HOMO. The occupied σ_s lies below the occupied bonding d states.

The fact that all doubly-degenerate dimer eigenstates are either fully occupied by two electrons or empty suggests that the MAE will be relatively low unless SOC leads to a reordering and a change in occupation of the levels close to the Fermi energy. For the Ni_2 dimer the SOC-induced splitting of the degenerate eigenstate for parallel orientation of the magnetic moments is modest; it is largest (0.13–0.17 eV) for the highest occupied $\delta_d^\star$ and δ_d states but the center of gravity of the SOC-split states remains essentially the same (see Fig. 2). In this case the one-electron energies are not a sufficient indicator of the easy axis of magnetization which must be derived from a full total-energy calculations. For both solutions the easy axis is determined by the larger orbital moment while the magnitude of the orbital anisotropy is of the same order of magnitude. The difficulty to find a unique answer for the MAE of the Ni dimer is related to the well-known fact that the description of the electronic ground state by a single-determinant wave function (which is inherent in DFT) fails for Ni where the ground state has a multideterminant character.[50] The two solutions differing in their orbital moments might be considered as possible single-determinant solutions while a better description might by achieved with an ansatz mixing these two (and possibly other) configurations.

For Pd_2 SOC induces a splitting of the degenerate $\delta_d^\star$ and δ_d states ranging between 0.29 and 0.36 eV, and a more modest splitting of the $\pi_d^\star$ and π_d states between 0.14 and 0.24 eV. The center of gravity of the SOC-split doublets can be shifted up or down; the very small MAE is the result of a very delicate balance of up and down shifts. For the hard axis (i.e., magnetization parallel to the dimer axis) we find,

in agreement with FSF (Ref. 8) and SCM (Ref. 7) but in disagreement with FKRE,[9] an almost vanishing orbital moment. For the hard (parallel) magnetic axis of the Pd_2 dimer, FSF (Ref. 8) report for both the LDA and the GGA a discontinuous change in the orbital magnetic moment from $\mu_L \sim 0$ to $\mu_L \sim 1.0\mu_B$ if the dimer bond length is increased beyond 2.50 Å while SCM (Ref. 7) report a similar increase in the orbital moment for a bond length compressed to 2.15 Å. We find in our GGA calculations the same discontinuous variation in the orbital moment as reported by FSF. If the bond length is only very slightly increased from its equilibrium value of 2.49–2.51 Å, the orbital moment increases to $\mu_L \sim 1.0\mu_B$ while the orbital moment along the easy axis is found to be rather insensitive to the dimer length. The discontinuous change in the orbital moment reverses the sign of the orbital anisotropy but in both GGA calculations the sign of the MAE remains the same; it even increases to a large value of about 50 meV (both FSF and present work). Only for the LDA calculations a reversal of the sign of the MAE is found if the bond length is stretched beyond 2.6 Å.[8] The discrepancy with respect to the work of FKRE is related to a very large bond length of 2.93 Å reported in their work—it is difficult to understand the origin of such a large Pd-Pd distance because the LDA used in their work rather tends to underestimate the bond lengths. FSF report an LDA value of the bond length of 2.45 Å, smaller than their GGA value as expected.

For Pt_2 we calculate large strongly anisotropic spin and orbital moments—$\mu_S = 1.88(1.34)\mu_B$, $\mu_L = 2.74(0.80)\mu_B$ for the easy (hard) magnetic axis. Pt_2 is the only dimer for which SOC influences also the bond length. In the scalar-relativistic mode we find $d = 2.33$ Å (at a magnetic moment of $\mu_S = 2\mu_B$); including SOC we calculate $d = 2.38$ Å for magnetization along the easy axis and $d = 2.35$ Å for hard-axis magnetization. No similar magnetostructural effect has been found for the other $5d$ dimers Ir_2 and Os_2. SOC leads to a reordering of the eigenstates close to the Fermi level even for perpendicular orientation of the magnetization [see Fig. 2(c)]—the $\sigma_d^\star$ state is lowered below the $\delta_d^\star$ state occupied by two electrons which is now the HOMO. The splitting of the doubly-degenerate $\pi_d^\star$ and $\delta_d^\star$ eigenstates at either side of the HOMO for a magnetization parallel to the dimer axis is larger than the separation of the eigenlevels. This leads to a change in occupation: one electron from a $\delta_d^\star$ state is transferred to the lower component of the $\pi_d^\star$ state; the HOMO is now the $\sigma_d^\star$ state as in the scalar-relativistic approximation. In addition, the pronounced anisotropy of the spin moment (and hence also of the exchange splitting) is reflected in the eigenvalue spectra—for some eigenstates SOC splitting is not symmetrical but accompanied by a shift in the center of gravity of the split eigenstates. This leads to contributions to the MAE of 46.3 meV which are not restricted to eigenstates close to the Fermi level. Similar effects have also been seen for Ir_2 and (although to a much smaller extent) for Os_2; they decrease with a decreasing orbital anisotropy.

C. Fe group

For the dimers of the Fe-group metals the trend in the MAE is rather complex. Fe_2 shows axial anisotropy but with

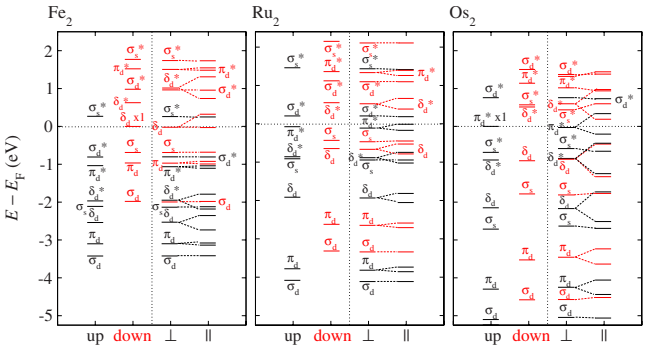

FIG. 3. (Color online) Kohn-Sham eigenvalue spectra for Fe_2 (left), Ru_2 (center), and Os_2 (right) dimers, cf. Fig. 1.

a very small MAE of only 0.32 meV, Ru_2 has perpendicular anisotropy with a large negative MAE of −36.5 meV, and Os_2 an axial anisotropy with a lower MAE of only 28.8 meV. Only for Fe_2, reference values from the work of FKRE (Ref. 9) are available; they find a much larger MAE (32 meV) related to a much higher orbital anisotropy.

The electronic ground-state configurations are s^2d^6 for Fe and Os but sd^7 for Ru. In the scalar-relativistic approximation the ground state is $S=3$ for the Fe dimer and $S=2$ for the Ru and Os dimers. For Ru_2 we have also found solutions with $S=1$ and a lower bond length of $d=2.03$ Å, and with $S=3$ solution and $d=2.23$ Å, both are 357 and 303 meV above the ground state, respectively. Despite these relatively large energy differences, it was found that different initializations of the magnetic moment in the fully relativistic calculations can lead to different locally stable solutions. Here we report only the results for the lowest energy. Differences in the atomic ground-state configurations and in the exchange splitting lead to different eigenvalue spectra. In the scalar-relativistic approximation (and also for perpendicular magnetization if SOC is included), the HOMO of the Fe_2 dimer is the doubly-degenerate minority δ_d state occupied by one electron only while the highest occupied majority state is the antibonding $\sigma_d^\star$ state (see Fig. 3). For the Ru dimer the HOMO is the doubly-degenerate antibonding majority $\pi_d^\star$ state occupied by two electrons while the highest occupied minority state is the σ_s state. For Os_2 the HOMO is again the $\pi_d^\star$ state but, because the relativistic effects shift the antibonding $\sigma_s^\star$ state (which is unoccupied for Ru_2) below the HOMO, it is now occupied only by one electron. Hence already in a scalar-relativistic mode, all three dimers have different electronic configurations close to the Fermi edge.

For the Fe_2 the spin moment is almost unchanged by SOC and the orbital magnetic moment is very small: $0.16\mu_B$ for the hard (perpendicular) axis and $0.32\mu_B$ for the easy (parallel) axis. For the hard axis the orbital moment agrees with FKRE (Ref. 9) but for the easy axis they report a much larger orbital moment. We find that the result for the orbital magnetic moment depends critically on the initialization of the magnetic moment. If for a magnetic moment parallel to the dimer axis the relativistic calculation is started with a lower initial spin moment, it converges to a state with the same spin moment but with a much larger orbital moment of $\mu_L = 1.74\mu_B$, i.e., very close to the value reported by FKRE. If

the iterations are continued (by setting a lower convergence criterion) the calculation converges to the solution with low orbital moment (which is lower in energy by about 86 meV). We also tried to find a high-μ_L solution for the hard axis but the calculations always converged to the low-moment result. SOC splits for a parallel magnetic axis the degenerate δ_d HOMO, but as the center of gravity is up shifted, the energy gain is very modest. As the changes in the lower-lying eigenstates are balanced, this explains the very small value of the MAE.

For Ru_2 we find zero orbital magnetic moment for a magnetization along the dimer axis (as for Pd_2), and a modest orbital moment for perpendicular orientation. SOC induces for axial orientation of the magnetic moment a splitting of the degenerate and fully occupied $\pi_d^\star$ HOMO by 0.12 eV, the lower-lying $\delta_d^\star$ and δ_d states are split by 0.20–0.26 eV, and the splitting is accompanied by an up shift of the center of gravity (see Fig. 3). The change in the sum of the one-electron energies is −40 meV; this correlates rather well with the calculated perpendicular MAE of −35.5 meV.

For the Os_2 dimer we calculate a spin anisotropy of $\Delta\mu_S=0.26\mu_B$ which is even larger than the orbital anisotropy of $\delta\mu_S=0.18\mu_B$. The axial anisotropy with MAE=29 meV results mainly from the splitting of the doubly-degenerate $\pi_d^\star$ HOMO occupied by only one electron. The SOC-induced splitting of the lower-lying π_d and δ_d levels is quite large but symmetric; the changes in all other eigenvalues essentially balance each other.

D. Post-DFT calculations

A certain weakness of the DFT is that the effective one-electron potential is orbital independent. To test whether an orbital dependence of the electron-electron interaction has a strong influence on the calculated orbital moments and magnetic anisotropy energies, we performed some calculations using a hybrid functional mixing Hartree-Fock (and hence orbital-dependent) exchange with DFT exchange in a ratio of 1:3 and treating correlation at the GGA level, and with a DFT+U approach[22,51] adding a Hubbard-type on-site Coulomb potential U acting on the d electrons to the DFT Hamiltonian. In the version of the DFT+U proposed by Dudarev *et al.*,[51] the on-site repulsion enters only in the form $(U-J)$, where J is the on-site exchange interaction. We use a constant value of $J=1$ eV and vary U between $U=1$ eV (representing the GGA limit—but note that there might be small differences arising from incomplete cancellations between the double-counting corrections in the standard DFT and Hubbard terms) and $U=5$ eV. The on-site repulsion increases the exchange splitting for the partially occupied d states but leaves the potential acting on fully occupied or empty eigenstates essentially unchanged. We use the DFT+U approach in the form of GGA+U calculations.

The use of the GGA+U is based on the observation of Chadov *et al.*[21] that with a value of $U\sim3$ eV for the bulk ferromagnets orbital moments in agreement with experiment are obtained while leaving the spin moment unchanged. The hybrid functional chosen is the HSE03 functional[47] (but the PBE0 functional[46] gives essentially identical results because the screening of the exchange in the HSE03 functional is long range and ineffective for isolated atoms and dimers). It must, however, be pointed out that for bulk ferromagnetic hybrid functionals lead to an overestimation of the spin moment.[52] For Fe the calculated moment is about $3\mu_B$, substantially larger than both experiment and conventional GGA calculations (which agree on a moment of $2.2\mu_B$). The results are compiled in Table II.

For Ni_2 we find that admixture of Hartree-Fock exchange increases the dimer bond length, leaves the spin moments unchanged, and leads even to a slight reduction in the orbital moment for easy-axis orientation (compared to the low-energy solution A in the GGA). Along the hard axis the orbital moment is unaffected. The MAE is reduced from 6.5 to 3.7 meV. In calculations with hybrid functionals we find only the solution with a substantial orbital moment for in-axis magnetization, in contrast to the GGA calculations.

HSE03 calculations for Pd_2 leave the bond length and the spin and orbital moments for parallel orientation of the magnetic moment unchanged; for perpendicular orientation the orbital moment is increased from $0.36\mu_B$ to $0.50\mu_B$. The MAE is very small; we find that a perpendicular orientation is still preferred but only by 0.3 meV.

In hybrid-functional calculations for Pt_2 the bond length is slightly increased by 0.05 Å. Spin moments are hardly affected but the orbital moment of the dimer increases from $2.74\mu_B$ to $3.02\mu_B$ for easy (parallel) orientation of the magnetic moment and from $0.80\mu_B$ to $1.06\ \mu_B$ for hard-axis orientation. The spin anisotropy is slightly reduced while the orbital anisotropy remains unchanged. The MAE is reduced from 46.5 to 30.5 meV.

Examination of the eigenvalue spectrum shows that the main effect of the admixture of a fraction of Hartree-Fock exchange is to increase the exchange splitting of the partially occupied eigenstates. For the Pt_2 dimer these are the $\pi_d^\star$ states where the exchange splitting is increased from 1.05 to 3.05 eV for the bonding π_d states the increase is from 0.86 to 1.90 eV. The influence is much smaller for the π- and σ-bonded d states and for the s states (all changes are smaller than 0.1 eV), whereas changes in the bonding/antibonding splitting are also modest. Although in the scalar-relativistic approximation the empty $\pi_d^\star$ state is pushed quite far above the Fermi level, due to a strongly increased SOC splitting of both the $\pi_d^\star$ and $\delta_d^\star$ states for in-axis orientation, we find a similar change in the occupation of the highest eigenstates as with the GGA functional (see Fig. 4 and compare with Fig. 2) and consequently only a reduction but no reversal of the MAE.

For Pd_2 the partially occupied d state is the antibonding $\sigma_d^\star$ state whose exchange splitting is increased to 3.32 eV but this does not introduce any change in the orbital occupancy; the perpendicular anisotropy is preserved. For Ni_2 the strongest increase in the exchange splitting is calculated for the antibonding $\delta_d^\star$ but, as the occupied majority-spin component is located at sufficiently high binding energy, this does not induce a change in the magnetic anisotropy.

We have also performed a few calculations with a GGA+U Hamiltonian and U varying between 1 and up to 5 eV.[51] The effect of the Hubbard-type on-site potential U is again to increase the exchange splitting of partially occupied eigen-

TABLE II. Interatomic distance d (in Å), spin μ_S and orbital μ_L moments (in μ_B) of transition-metal dimers for axial and perpendicular orientations of the magnetization, MAE, and spin-orbit coupling constant ξ (both in meV). The MAE is positive for any easy axis parallel to the dimer axis. The calculations have been performed with a hybrid functional.

			Axial		Perp.			
Dimer	Method	d	μ_S	μ_L	μ_S	μ_L	MAE	ξ
Ni_2	HSE03	2.27	1.98	0.50	1.96	0.30	3.7	101
	GGA+U(1 eV) (A)	2.09	1.98	0.54	1.98	0.38	9.2	101
	GGA+U(1 eV) (B)	2.08	1.98	0.02	1.98	0.38	−6.7	117
	GGA+U(2 eV) (A)	2.08	1.98	0.48	1.98	0.38	25.0	105
	GGA+U(2 eV) (B)	2.07	1.98	0.02	1.98	0.38	−6.4	117
	GGA+U(3 eV) (A)	2.08	2.00	0.42	2.00	0.36	17.0	114
	GGA+U(3 eV) (B)	2.07	1.98	0.02	2.00	0.36	−6.2	117
Pd_2	HSE03	2.50	1.96	0.02	1.98	0.50	−0.3	343
	GGA+U(1 eV)	2.49	1.96	0.02	1.98	0.62	−2.3	393
	GGA+U(3 eV)	2.50	1.94	0.02	1.98	0.40	−2.1	384
	GGA+U(5 eV)	2.50	1.94	0.04	1.98	0.40	−2.3	355
Pt_2	HSE03	2.43	1.88	3.02	1.28	1.06	30.5	743
	GGA+U(1 eV)	2.38	1.88	2.74	1.34	0.80	45.6	735
	GGA+U(2 eV)	2.38	1.90	2.82	1.40	0.84	13.3	708
	GGA+U(3 eV)	2.38	1.90	2.90	1.48	0.88	−19.5	644
	GGA+U(5 eV)	2.37	2.04	3.12	1.66	1.00	−85.0	492

states. For the Ni_2 we find for an axial orientation of the magnetization, as for the standard GGA calculations, the coexistence of solutions with high and almost vanishing orbital moment, leading to a positive and negative MAE, respectively. The solution with an easy axis parallel to the dimer axis (positive MAE) is lower in energy, independent of the value of U, with an energy difference varying between 17 and 28 meV. A modest on-site Coulomb potential leads to a slightly stronger MAE. Since this is accompanied by a decrease in the orbital anisotropy, this cannot be described by a perturbative approach. For Pd_2 only the solution with almost zero orbital moment exists for parallel magnetization, independent of U. Since there is also only a modest decrease in the perpendicular orbital moment with increasing U, the MAE is hardly affected.

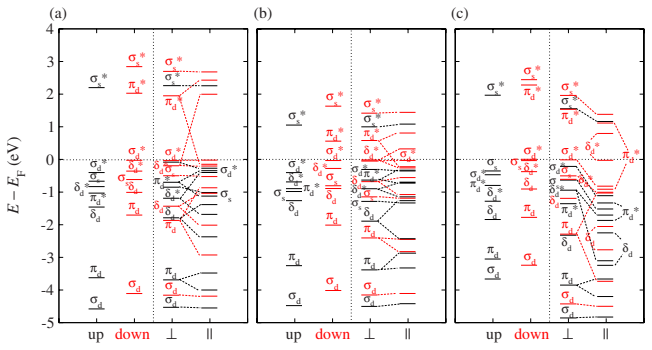

FIG. 4. (Color online) Kohn-Sham eigenvalue spectra for Pt_2 dimers for parallel and perpendicular orientations of the magnetic moments, calculated using (a) a hybrid functional and with a GGA+U approach, and (b) U=2 eV and (c) U=5 eV (cf. Fig. 2).

For the Pt dimer the GGA+U calculations predict a change in sign of the MAE with an increasing Coulomb repulsion. At a modest value of U=2 eV, the main effects are enhanced spin and orbital moments, an increased exchange splitting of the $\pi_d^\star$ states, and an increased SOC splitting—due to their combined effect, the ordering of the eigenstates near the Fermi level remains essentially the same for both axial and perpendicular orientations of the magnetization. As a result, the easy axis remains unchanged but due to shifts of lower-lying eigenstates, the MAE is reduced (see Fig. 4). For U=5 eV, the exchange splitting of the $\pi_d^\star$ states (Δ_{ex}=2.8 eV) and π_d(Δ_{ex}=1.5 eV) is increased to about the same magnitude as with the hybrid functional. For these states we also find a very large SOC splitting—even larger for the bonding component than calculated with a hybrid functional while the SOC splitting of the $\delta_d^\star$ state remain more modest. These lead to a rearrangement of the occupied eigenstates even at higher binding energies and to significant changes also in other contributions to the total energy, beyond the one-electron energies.

E. Dimers vs monowires

It is also interesting to confront our results for the magnetic properties of transition-metal dimers with the results available in the literature[30–32] for straight monowires. These results are compiled in Table III. The comparison shows that the relation between dimers and wires is entirely different for the magnetic 3d metals and for the nonmagnetic 4d and 5d metals.

For the 3d elements the interatomic distance is considerably shorter in a dimer than in an infinite monowire. The

TABLE III. Comparison of the magnetic properties of dimers and monowires: interatomic distance d (in Å), spin μ_S, and orbital μ_L moments (in μ_B) for axial and perpendicular orientations of the magnetization, and MAE (in meV/atom). The MAE is positive for any easy axis parallel to the dimer axis.

			Axial		Perp.		
Element		d	μ_S	μ_L	μ_S	μ_L	MAE
Fe_2	Dimer	1.98	2.92	0.16	2.92	0.08	0.15
Fe[a]	Wire	2.25	3.45	0.44	3.45	0.08	2.25
Co_2	Dimer	1.96	1.95	0.39	1.95	0.16	3.55
Co[a]	Wire	2.15	2.12	0.10	2.12	0.08	−0.68
Ni_2	Dimer	2.09	0.99	0.29	0.98	0.19	3.25
Ni[a]	Wire	2.18	1.20	0.50	1.20	0.06	11.43
Ru_2	Dimer	2.07	1.99	0	1.97	0.12	−18.25
Ru[b]	Wire	2.24	1.12	0.15	1.10	0.03	−10.50
Rh_2	Dimer	2.21	1.93	0.91	1.90	0.25	23.65
Rh[b]	Wire	2.31	0.30	0.36	0	0	5.00
Pd_2	Dimer	2.49	0.98	0.01	0.99	0.18	−1.15
Pd[b]	Wire	2.48	0.50	0	0.30	0.12	−5.00
Pt_2	Dimer	2.38	1.88	2.74	1.34	0.80	23.15
Pt[c]	Wire	2.39	0.19	0.17	0	0	2.00

[a]Reference 31, GGA.
[b]Reference 30, LSDA.
[c]Reference 32, GGA.

increased distance leads to an enhancement of the spin moment but not necessarily to a corresponding enhancement of the orbital moment. For the 4d and 5d elements the contraction of the bond length in the dimer is much more modest; for Pd and Pt it is the same in the dimer and in the infinite wire. Both spin and orbital moments are strongly reduced in the wire compared to the dimer.

The formation of orbital moments and the origin of a strong MAE in monowires has been discusses by Mokrousov *et al.*,[30] Smogunov *et al.*,[32] and Velev *et al.*[53] in terms very similar to the analysis we have used for dimers. The main difference is that the discrete eigenvalue spectrum of the dimer is replaced by a set of one-dimensional bands with sharp van-Hove singularities at the upper and lower edges (see, e.g., Spišák and Hafner,[26] and Mokrousov *et al.*[30] for detailed representations of the one-dimensional band structure). Under the rotational symmetry (group $C_{\infty v}$) of the wire there are two double-degenerate bands (corresponding to the π_d and δ_d states of the dimer) and a nondegenerate band (corresponding to the σ_d states). The bands are split under the influence of exchange and spin-orbit interactions. The SO splitting depends again on the direction of magnetization; for parallel magnetization the splitting of the doublets is first order in the SOC operator; for perpendicular magnetization the SOC operator has zero matrix elements within the doublets; a splitting occurs only near the band crossing points.[53] A spin moment is formed when the exchange splitting leads to a larger occupation of spin-up states while an orbital moment is formed if bands with angular momenta $\pm\mu_l$ have different occupancies. A strong effect is to be expected if the van-Hove singularity of a spin-split degenerate band occurs close to the Fermi edge.

The essential difference between the 3d and the heavier metals is that in the former case the exchange splitting is much larger than the SOC splitting while for the second group both are of similar magnitude. For the 3d elements the band narrowing resulting from the increased interatomic distance in the wire leads to an enhanced spin moment. For Fe wires the Fermi level lies just above the lower van-Hove singularity of the minority δ_d band (corresponding to the δ_d state of the dimer), while for Ni wires it lies just above the upper singularity (corresponding to the δ_d^* state of the dimer). In these cases, the SOC-induced splitting is more efficient for the wire with large density of states (DOS) even at E_F, leading to an increased orbital moment for parallel but not for perpendicular magnetization. In a Co wire the Fermi level falls close to the DOS minimum in the δ_d band; in this case the orbital moments in the wire is even lower than in the dimer. For the heavy elements the bandwidths of the wire are strongly influenced by long-range interactions—this leads to a strong decrease in the exchange splitting and of the spin moment if the interatomic distance is lower than a critical value.[30] For all wires the equilibrium interatomic spacing is lower than this threshold; the onset of the formation of an orbital moment is coupled to the formation of a spin moment.[30,32] Hence for these elements the orbital moment in an infinite wire is decreased compared to the dimer and this is also reflected in the magnitude of the MAE. The sign of the MAE is the same for dimers and wires except for Co where the strong decrease in the orbital anisotropy leads to a small negative MAE for the infinite wire.

IV. DISCUSSION AND CONCLUSIONS

We have presented detailed DFT calculations of the influence of spin-orbit coupling (SOC) on the structural and magnetic properties, and of the magnetic anisotropy energies of dimers of metals from groups 8 to 10 of the Periodic Table. For the metals from group 10 we have also briefly examined the influence of orbital-dependent post-DFT corrections (mixing of Hartree-Fock and DFT exchange, and addition of an orbital-dependent on-site Coulomb potential to correct for the self-interaction error in DFT).

SOC has almost no influence on the dimer bond length. Only for a Pt_2 dimer a stretching of the Pt-Pt distance by 0.03 Å has been found. Due to the mixing of different spin eigenstates, the spin moment is no longer an integer multiple of μ_B when SOC is included. For all dimers considered here, SOC induces a slight reduction in the spin moment by $0.02\mu_B$–$0.25\mu_B$, increasing with the strength of the SOC. For the heavier elements the coupling between spin and orbital moments also induces an anisotropy of the spin moments which is modest for the 4d and rather strong for the 5d elements. In some cases, the determination of the relativistic ground state is hampered by the existence of multiple local minima with different orbital moments. This is the case for Ni_2 where, for a magnetic axis parallel to the dimer axis, a solution with a large orbital moment is only 27 meV lower in energy than a low-moment solution while for perpendicular

magnetization, only one solution with an intermediate value of the orbital moment is found. Hence the two solutions lead to different signs of the orbital anisotropy and of the MAE. This could also explain why DFT calculations published in the literature predict different easy-axis orientations.[7,9] For a Pd_2 dimer we find, in agreement with earlier results,[8] a discontinuous variation in the orbital moment with the length of the dimer. A further difficult case is the Fe_2 dimer. Here our result for the easy-axis orbital moment and for the MAE is much lower than the value reported by Fritsch *et al.*[9]—here again we succeeded in finding a high-moment solution but at a higher energy than the low-moment results. Altogether our analysis has demonstrated that very strict convergence criteria and a careful exploration of the potential-energy surface as a function of both spin and orbital moments is required for a reliable determination of the MAE.

One of the main objectives of our study was to elucidate the physical mechanism determining the variation in the MAE with *d*-band filling and strength of the SOC. Here we found that the analysis of the eigenvalue spectra proposed by Strandberg *et al.*[7] is very useful. For all three dimers of the Co group, the HOMO in a scalar-relativistic approximation and for perpendicular magnetization if SOC is included is a doubly-degenerate $\delta_d^\star$ state occupied by a single electron. In this case the most important factor leading to a preferred axial magnetization is the lifting of the degeneracy of the eigenstates leading to a reduction in the one-electron energies. For the dimers from the Fe and Ni groups, we find a small axial anisotropy for the 3*d* dimers, perpendicular anisotropy for the 4*d* dimers, and a rather large axial MAE for the 5*d* dimers. In these cases we could show that a decisive factor is difference in the atomic ground states (lower *d*-electron number) of the 4*d* elements. For both Ru_2 and Pd_2 the HOMO is a doubly-degenerate doubly occupied $\pi_d^\star$ state and SOC splitting stabilizes a perpendicular anisotropy as discussed in detail above. For the other four dimers an axial anisotropy is calculated.

Post-DFT calculations have been explored for the dimers of the Ni group. Mixing orbital-dependent Hartree-Fock with DFT exchange leads to an increased bond length for Ni and Pt dimers, in which spin moments remain unaffected, while orbital moments are slightly increased for Pd and Pt—but this hardly affects the MAE, adding an on-site Coulomb *U* to the *d* states. Similarly to an exact-exchange contribution, the effect of *U* is to increase the exchange splitting of the partially occupied *d* states and an increase in the SOC. Spin moments are hardly changed; orbital moments decrease with increasing *U* for Ni_2 and Pd_2 but increase for Pt_2 where a large *U* leads to a change in sign of the MAE. However, such large values of the on-site repulsion evidently lead to a rather unrealistic eigenvalue spectrum.

We also presented a comparative analysis of the formation of orbital moments and of MAEs in dimers and in infinite straight monowires. It is shown that the differences in the magnetic properties of dimers and wires can be traced back to the difference between the discrete eigenvalue spectrum of the dimer and a continuous one-dimensional DOS of the wire. This analysis also highlights the difference between the magnetic 3*d* and the nonmagnetic 4*d* and 5*d* elements.

In summary, we have presented detailed DFT calculations of the magnetic anisotropy energies of dimers of the late transition atoms from groups 8 to 10, providing an improved understanding of the physical effects determining the sign and magnitude of the MAE. Our results also illustrate some of the difficulties inherent in such calculations, associated with the difficulty of finding the relevant minima on a complex potential-energy surface and explaining certain discrepancies with regard to other calculations.[7–9] Calculations with hybrid functionals and a GGA+*U* Hamiltonian (which introduce an orbital dependence of the effective one-electron potential) introduce only modest changes with respect to conventional DFT calculations, as long as only moderate realistic values of the on-site Coulomb repulsion are admitted. The largest MAE calculated for a Pt_2 dimer corresponds to a temperature of about 500 K. However, whether this is a result that is significant for potential applications will depend on the ability to find a substrate or matrix supporting the dimer without strongly reducing the MAE.

ACKNOWLEDGMENT

This work has been supported by the Austrian Science Funds under Project. No. P19712-N16.

*Corresponding author; juergen.hafner@univie.ac.at

[1] D. Sellmyer and R. Skomski, *Advanced Magnetic Nanostructures* (Springer, New York, 2006).
[2] S. Maekawa and T. Shinjo, *Spin Dependent Transport in Magnetic Structures* (Taylor & Francis, London, 2002).
[3] J. A. Alonso, Chem. Rev. (Washington, D.C.) **100**, 637 (2000).
[4] F. Baletto and R. Ferrando, Rev. Mod. Phys. **77**, 371 (2005).
[5] T. Futschek, M. Marsman, and J. Hafner, J. Phys.: Condens. Matter **17**, 5927 (2005).
[6] T. Futschek, J. Hafner, and M. Marsman, J. Phys.: Condens. Matter **18**, 9703 (2006).
[7] T. O. Strandberg, C. M. Canali, and A. H. MacDonald, Nature Mater. **6**, 648 (2007); Phys. Rev. B **77**, 174416 (2008).
[8] L. Fernandez-Seivane and J. Ferrer, Phys. Rev. Lett. **99**, 183401 (2007); **101**, 069903(E) (2008).
[9] D. Fritsch, K. Koepernik, M. Richter, and H. Eschrig, J. Comput. Chem. **29**, 2210 (2008).
[10] B. Lazarovits, L. Szunyogh, and P. Weinberger, Phys. Rev. B **67**, 024415 (2003).
[11] B. Nonas, I. Cabria, R. Zeller, P. H. Dederichs, T. Huhne, and H. Ebert, Phys. Rev. Lett. **86**, 2146 (2001).
[12] I. Cabria, B. Nonas, R. Zeller, and P. H. Dederichs, Phys. Rev. B **65**, 054414 (2002).
[13] S. Bornemann, J. Minar, J. B. Staunton, J. Honolka, A. Enders, K. Kern, and H. Ebert, Eur. Phys. J. D **45**, 529 (2007).
[14] P. Bruno, Phys. Rev. B **39**, 865 (1989).
[15] G. van der Laan, J. Phys.: Condens. Matter **10**, 3239 (1998).
[16] C. Andersson, B. Sanyal, O. Eriksson, L. Nordström, O. Karis,

D. Arvanitis, T. Konishi, E. Holub-Krappe, and J. H. Dunn, Phys. Rev. Lett. **99**, 177207 (2007).
[17] I. V. Solovyev, Phys. Rev. Lett. **95**, 267205 (2005).
[18] M. S. S. Brooks, Physica B & C **130**, 6 (1985).
[19] O. Eriksson, M. S. S. Brooks, and B. Johansson, Phys. Rev. B **41**, 7311 (1990).
[20] H. Eschrig, M. Sargolazei, K. Koepernik, and M. Richter, Europhys. Lett. **72**, 611 (2005).
[21] S. Chadov, J. Minar, M. I. Katsnelson, H. Ebert, D. Ködderitzsch, and A. I. Lichtenstein, Europhys. Lett. **82**, 37001 (2008).
[22] V. I. Anisimov, J. Zaanen, and O. K. Andersen, Phys. Rev. B **44**, 943 (1991).
[23] G. Kotliar, S. Y. Savrasov, K. Haule, V. S. Oudovenko, O. Parcollet, and C. A. Marinetti, Rev. Mod. Phys. **78**, 865 (2006).
[24] P. Söderlind, O. Eriksson, B. Johansson, R. C. Albers, and A. M. Boring, Phys. Rev. B **45**, 12911 (1992).
[25] W. D. Brewer, A. Scherz, C. Sorg, H. Wende, K. Baberschke, P. Bencok, and S. Frota-Pessoa, Phys. Rev. Lett. **93**, 077205 (2004).
[26] D. Spišák and J. Hafner, Phys. Rev. B **66**, 052417 (2002); **67**, 214416 (2003).
[27] Y. Mokrousov, G. Bihlmayer, S. Blügel, and S. Heinze, Phys. Rev. B **75**, 104413 (2007).
[28] M. Komelj, C. Ederer, J. W. Davenport, and M. Fähnle, Phys. Rev. B **66**, 140407(R) (2002).
[29] C. Ederer, M. Komelj, and M. Fähnle, Phys. Rev. B **68**, 052402 (2003).
[30] Y. Mokrousov, G. Bihlmayer, S. Heinze, and S. Blügel, Phys. Rev. Lett. **96**, 147201 (2006).
[31] J. C. Tung and G. Y. Guo, Phys. Rev. B **76**, 094413 (2007).
[32] A. Smogunov, A. dal Corso, A. Delin, R. Weht, and E. Tosatti, Nat. Nanotechnol. **3**, 22 (2008).
[33] M. C. Desjonquères, C. Barreteau, G. Autès, and D. Spanjaard, Eur. Phys. J. B **55**, 23 (2007).
[34] G. Kresse and J. Furthmüller, Comput. Mater. Sci. **6**, 15 (1996); Phys. Rev. B **54**, 11169 (1996).
[35] G. Kresse and D. Joubert, Phys. Rev. B **59**, 1758 (1999).
[36] J. P. Perdew and Y. Wang, Phys. Rev. B **45**, 13244 (1992).
[37] S. H. Vosko, L. Wilk, and M. Nusair, Can. J. Phys. **58**, 1200 (1980).
[38] E. G. Moroni, G. Kresse, J. Hafner and J. Furthmüller, Phys. Rev. B **56**, 15629 (1997).
[39] P. E. Blöchl, Phys. Rev. B **50**, 17953 (1994).
[40] G. Kresse and O. Lebacq, *VASP Manual* http://cms.mpi.univie.ac.at/vasp/vasp/vasp.html.
[41] L. Kleinman, Phys. Rev. B **21**, 2630 (1980).
[42] A. H. MacDonald, W. E. Pickett, and D. D. Koelling, J. Phys. C **13**, 2675 (1980).
[43] D. Hobbs, G. Kresse, and J. Hafner, Phys. Rev. B **62**, 11556 (2000).
[44] M. Marsman and J. Hafner, Phys. Rev. B **66**, 224409 (2002).
[45] G. Y. Guo, W. M. Temmermann, and H. Ebert, J. Phys.: Condens. Matter **3**, 8205 (1991).
[46] J. P. Perdew, M. Ernzerhof, and K. Burke, J. Chem. Phys. **105**, 9982 (1996); K. Burke, M. Ernzerhof, and J. P. Perdew, Chem. Phys. Lett. **265**, 115 (1997).
[47] J. Heyd, G. E. Scuseria, and M. Ernzerhof, J. Chem. Phys. **118**, 8207 (2003); J. Heyd and G. E. Scuseria, *ibid.* **120**, 7274 (2004).
[48] J. Paier, M. Marsman, K. Hummer, G. Kresse, I. C. Gerber, and J. G. Angyan, J. Chem. Phys. **124**, 154709 (2006).
[49] A. Rohrbach, J. Hafner, and G. Kresse, Phys. Rev. B **69**, 075413 (2004).
[50] J. Bünemann, F. Gebhard, and W. Weber, in *Frontiers in Magnetic Materials*, edited by A. Narlikar (Springer, Berlin, 2005).
[51] S. L. Dudarev, G. A. Botton, S. Y. Savrasov, C. J. Humphreys, and A. P. Sutton, Phys. Rev. B **57**, 1505 (1998).
[52] A. Stroppa, K. Termentzidis, J. Paier, G. Kresse, and J. Hafner, Phys. Rev. B **76**, 195440 (2007).
[53] J. Velev, R. F. Sabirianov, S. S. Jaswal, and E. Y. Tsymbal, Phys. Rev. Lett. **94**, 127203 (2005).